AD-A041 102 NORTHWESTERN UNIV EVANSTON ILL DEPT OF MATERIALS SCIENCE F/G 14/2
GEOMETRICAL PROBLEMS WITH A POSITION SENSITIVE DETECTOR EMPLOYE--ETC(U)
JUN 77 M R JAMES, J B COHEN N00014-75-C-0580
UNCLASSIFIED TR-18 NL

1 OF 1
AD
A041102

END

DATE
FILMED
7-77

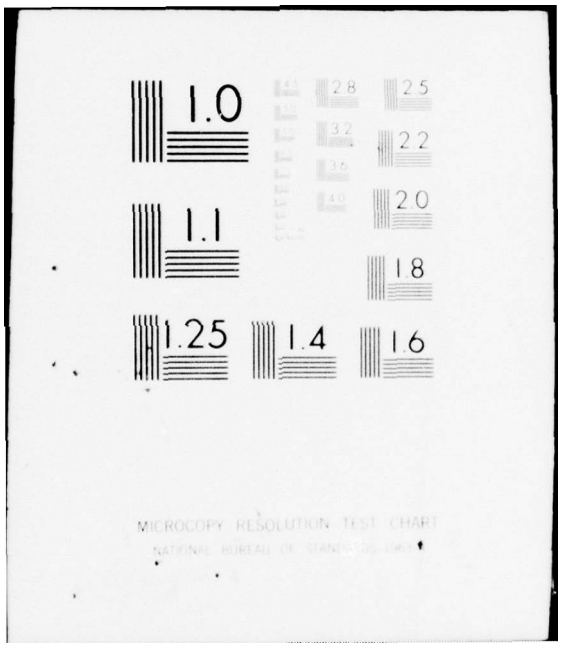
1.0
1.1
1.25
1.4
1.6
2.8
2.5
3.2
2.2
3.6
2.0
4.0
1.8
MICROCOPY RESOLUTION TEST CHART
NATIONAL BUREAU OF STANDARDS-1963-A

AD A041102

12
B.S.

NORTHWESTERN UNIVERSITY

DEPARTMENT OF MATERIALS SCIENCE

Technical Report No. 18
June 15, 1977

Office of Naval Research
Contract N00014-75-C-0580
NR 031-733

GEOMETRICAL PROBLEMS WITH A POSITION SENSITIVE DETECTOR EMPLOYED ON A DIFFRACTOMETER: ITS USE IN THE MEASUREMENT OF STRESS

by

M. R. James and J. B. Cohen

Distribution of this Document is Unlimited.

Reproduction in whole or in part is permitted for any purpose of the United States Government.

DDC
JUN 29 1977
C

EVANSTON, ILLINOIS

AD No.
DDC FILE COPY

(See form 1473

GEOMETRICAL PROBLEMS WITH A POSITION SENSITIVE DETECTOR EMPLOYED ON A DIFFRACTOMETER: ITS USE IN THE MEASUREMENT OF STRESS

M. R. James and J. B. Cohen

Northwestern University

Evanston, Illinois 60201

ABSTRACT

Defocussing errors associated with the use of a straight one dimensional position sensitive detector on a diffractometer are examined. Over a $10^\circ 2\theta$ range the error is $0.02^\circ 2\theta$ at worst.

GEOMETRICAL PROBLEMS WITH A POSITION SENSITIVE DETECTOR EMPLOYED ON A DIFFRACTOMETER: ITS USE IN THE MEASUREMENT OF STRESS

1. INTRODUCTION

In measurements of lattice strain a modified form of Seeman-Bohlin geometrical conditions for focusing are employed.* This permits a divergent primary beam and hence illumination of a considerable area of the specimen, yet results in a sharp diffracted beam at the focal point. The focusing circle defined by the target, specimen and receiving slit as shown in Fig. 1. is related to the radius of the diffractometer circle, R_{GC}, as follows[108]:

$$R_{FC} = R_{GC}/2\sin(\theta+\psi) \qquad 1.$$

Where ψ is defined in Fig. 1.b., Fig. 1. illustrates two possible conditions. For $\psi = 0$, the focal point lies on the goniometer circle at all 2θ angles. This is termed symmetrical or Bragg-Brentano focusing. A receiving slit placed on the 2θ arm at the position of the goniometer circle is always at the point of focus. For ψ not equal to zero, the point of focus

---

*As pointed out by Kunze[109] the usual symmetric or Bragg-Brentano arrangement is geometrically (though not mechanically) equivalent to a Seeman-Bohlin arrangement with $\psi=0$. Residual stress measurements usually employ the mechanical movement of the Bragg-Brentano diffractometer with the geometrical conditions of Seeman-Bohlin focusing.

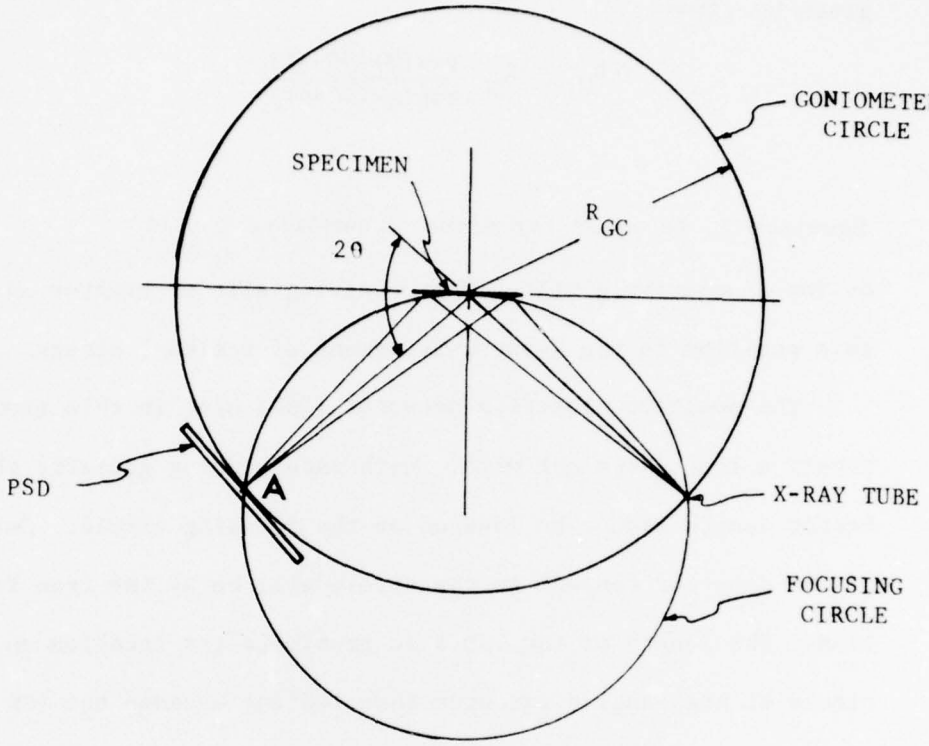

FIG. 1-A $\psi=0^{\circ}$

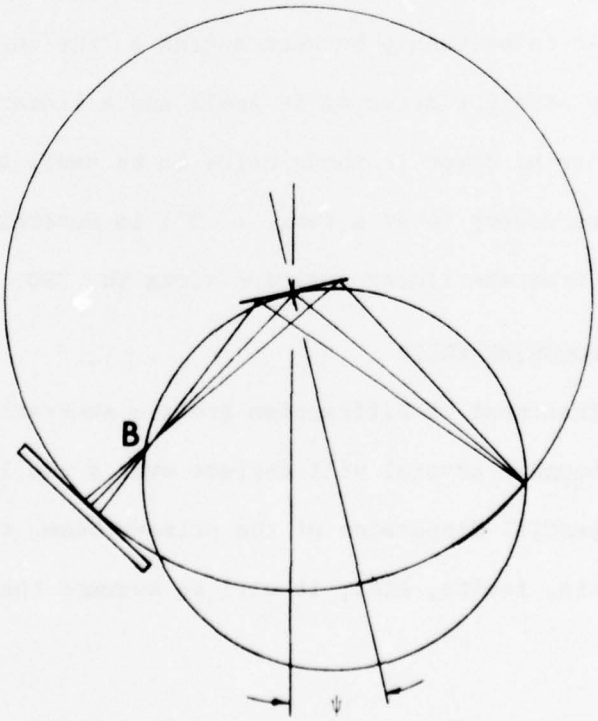

FIG 1-B $\psi=\psi^{\circ}$

FIGURE 1 Geometry of the focusing error with a PSD.

changes to point B in Fig. 1.b. The distance from the sample to B is given by (108):

$$R_p = R_{GC} \frac{\cos(\psi+(90-\theta))}{\cos(\psi-(90-\theta))} \quad . \qquad 2.$$

Equation 2. is valid for either a positive ψ tilt or for a negative ψ tilt. The receiving slit or counter may be moved to this position in the X-ray measurement of residual stress.

The position sensitive detector (PSD) used in this study is effectively a long, straight wire. With parafocusing geometry the entire detector length cannot be located on the focusing circle. Only that portion of the detector tangent to the circle will be at the true focusing position. The length of the PSD also prohibits its location on the focusing circle at high angles (greater than 140° 2θ) because the PSD is obstructed by the X-ray source on most diffractometers.

In the Appendix it was shown that for peak shifts less than 3° 2θ, the non-linear relationship between angles on the curved focusing circle and along the straight detector is small and a linear relation can be used. The defocusing error is shown below to be small so that correction factors are not necessary (over a range of 3°) in determining the true angular position from the linear position along the PSD.

2. DEFOCUSING ERROR

2.1. Treatment of Diffraction Profile Aberrations

Although ε crystal will reflect over a small range of 2θ depending on the spectial dispersion of the primary beam, the crystallite size, microstrain, faults, etc., it will be assumed that there is only one

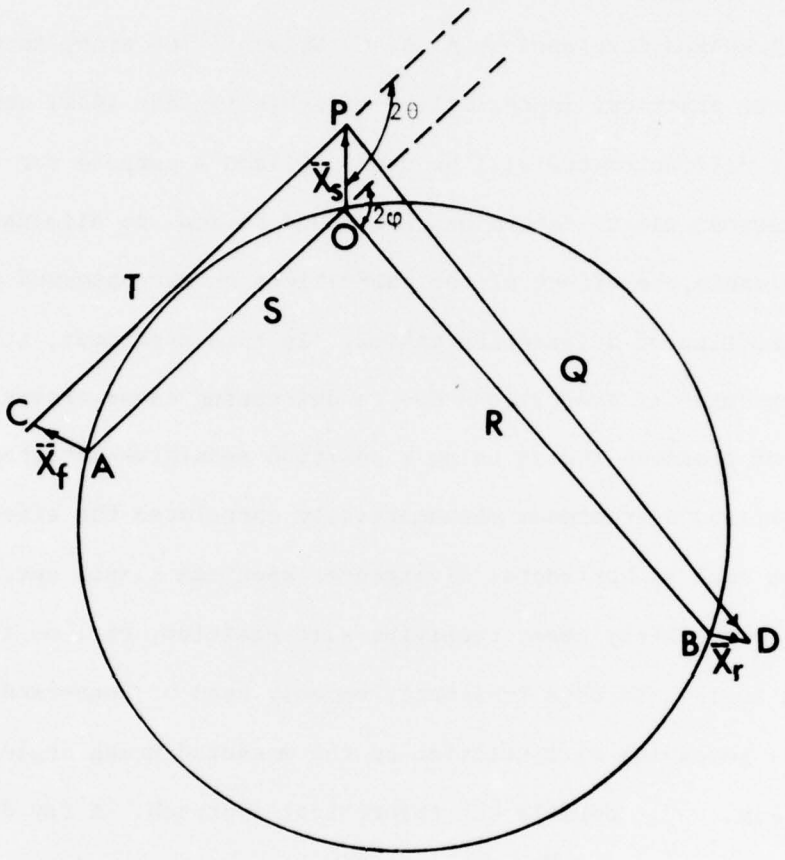

FIGURE 2 Geometry of the powder diffractometer.

wavelength and that Bragg's law applies exactly. For any hkl plane the diffraction angle is fixed.

A method developed by A. J. C. Wilson[110] to study aberrations arising from the practical impossibility of achieving the ideal arrangement in powder diffractometry will be used. Wilson's purpose for treating these aberrations was to determine what could be done to eliminate,as far as practicable,the effect of the aberrations on the observed positions, breadths and profiles of diffraction maxima. In this treatment, it is desired solely to determine if aberrations due to defocusing cause errors in the measurement of residual stress using a position sensitive detector.

Wilson's treatment mathematically correlates the effect of each aberration such as horizontal divergence, specimen shape, specimen transparency to the X-ray beam, receiving slit position, etc. on the measured Bragg angle. In this treatment, we only need be concerned with the effect of the receiving slit position on the measured Bragg angle.

Fig. 2. details the theoretical approach. A ray diverging from point C, a distance $\bar{X}_f$ from A, the centroid of the source, is diffracted at point P in the specimen a distance $\bar{X}_s$ from O, (the ideal position of the specimen), and passes through the receiving slit at D, at distance $\bar{X}_r$ from B, the point at which rays would be focused under ideal conditions. The main concern here for a PSD is with errors associated with the vector $\bar{X}_r$. The other missettings are included because of possible cross terms involving $\bar{X}_f$ and $\bar{X}_s$.

Following Wilson's coordinate system, unit vectors may be chosen with

$\tilde{i}$ and $\tilde{j}$ in the equatorial plane, $\tilde{i}$ radially outward from the focusing circle, $\tilde{j}$ tangential to the focusing circle, and $\tilde{k}$ axial. The $\tilde{X}$ direction is thus normal to the circle and $\tilde{Y}$ and $\tilde{Z}$ are tangential to it. Orthogonal components for the small vectors x_f, x_s, x_r may be chosen so that (see Fig. 2.),

x_s, y_s, z_s are parallel to $\tilde{i}, \tilde{j}, \tilde{k}$

x_f, and y_f are equatorial and respectively parallel and perpendicular to $\bar{S}$ in Fig. 2. and z_f is parallel to $\tilde{k}$

x_r, and y_r are equatorial and respectively parallel and perpendicular to $\bar{R}$, and z_r is parallel to $\tilde{k}$

Let 2ε represent the error in 2θ due to the aberrations. Then

$$2\theta = 2\varphi + 2\varepsilon \qquad 3.$$

where the angular reading on the diffractometer is actually 2φ. To calculate 2ε:

$$\cos 2\varphi - \cos 2\theta = \cos 2\varphi - \cos(2\varphi + 2\varepsilon) \qquad 4.$$

$$= 2\varepsilon \sin 2\varphi$$

or

$$2\varepsilon = [\cos 2\varphi - \cos 2\theta]/\sin 2\varphi \qquad 5.$$

where 2ε is in radians. Letting $\cos 2\varphi - \cos 2\theta = \delta$ this term can be separated into its components:

$$\delta = \delta_f + \delta_r + \delta_s + \delta_{fr} + \delta_{fs} + \delta_{rs} \qquad 6.$$

where δ_f, δ_r, δ_s represent the scalar components involving only the focal spot, receiving slit, and specimen respectively. δ_{fr}, δ_{fs}, and δ_{rs} are cross terms involving the designated constituents. These cross terms represent the correlation of one aberration on the others. For instance, if the

focal spot and effective diffracting position were perfectly positioned with the angular divergence of the beam being extremely small, there would be no receiving slit missetting because the diffracted beam would be a straight line. The receiving slit could be placed anywhere along this line. The correlation of the focal spot and receiving slit and specimen position and receiving slit must be accounted for. As the present concern is only with terms involving the receiving slit:

$$\delta = \delta_r + \delta_{fr} + \delta_{rs} \qquad 7.$$

The scalar terms as derived by Wilson are:

$$\delta_r = R^{-2}\sin 2\varphi[Ry_r - x_r y_r + \tfrac{1}{2}(y_r^2 + z_r^2)\cot 2\varphi + \ldots] \qquad 8.$$

$$\delta_{fr} = (RS)^{-1}(y_f y_r \cos 2\varphi + z_f z_r) \qquad 9.$$

$$\begin{aligned}\delta_{rs} = R^{-2}[&-x_r x_s \cos(2\varphi-\psi)\sin 2\varphi - y_r y_s \cos(2\varphi-\psi)\sin 2\varphi \\ &- x_r y_s \sin(2\varphi-\psi)\sin 2\varphi - z_r z_s(\cos 2\varphi + \tfrac{R}{S}) + \\ &- y_r y_s(\cos\psi + \tfrac{R}{S}\cos\psi\cos 2\varphi)]\end{aligned} \qquad 10.$$

Some of the scalar components are an order of magnitude smaller than others so the cross terms may be neglected. The term y_r represents the missetting of the receiving slit normal to the vector R in Fig. 2. For a PSD this term is given by the spatial resolution of the detector and is small, therefore terms involving $y_r y_f$ and $y_r y_s$ and $y_r x_s$ can be neglected since y_f, y_s, and x_s are also very small. From Eq. 5. and Eq. 7.

$$2\epsilon_r = (\delta_r + \delta_{rf} + \delta_{rs})/\sin 2\varphi \qquad 11.$$

Neglecting the axial divergence terms because the PSD slit height is small (3mm , equal to 1.2° for a diffractometer of radius 14.55 cm):

$$\begin{aligned}2\epsilon_r = R^{-2}[&Ry_r - x_r y_r + \frac{y_r^2}{2}\frac{\cot 2\varphi}{\sin 2\varphi} - x_r x_s \cos(2\varphi-\psi) \\ &- x_r y_s \sin(2\varphi-\psi)\end{aligned} \qquad 12.$$

The displacement is found by averaging $2\epsilon_r$ over the focal spot, specimen, and receiving slit. Neither x_r and x_s nor x_r and y_s are correlated, thus:

$$2\epsilon_r = R^{-2}[R\langle y_r\rangle - \langle x_r\rangle\langle y_r\rangle + \frac{\langle y_r^2\rangle}{2}\frac{\cot 2\varphi}{\sin 2\varphi} - \langle x_r\rangle\langle x_s\rangle\cos(2\varphi-\psi)$$

$$- \langle x_r\rangle\langle y_s\rangle \sin(2\varphi-\psi)] \qquad 13.$$

where $\langle x_r y_r\rangle = \langle x_r\rangle\langle y_r\rangle$ is assumed. Now $\langle x_s\rangle = x_s$ as x_s is approximately constant for a flat specimen.* If the center of gravity of the illuminated area lies on the axis of rotation of the specimen, $\langle y_s\rangle = 0$. This is never possible because of the variation in intensity across the beam, but the average is still small. Both x_r and y_r will be functions of 2φ and the position of the PSD. Formulations for each are derived.

2.2. Derivation of $\langle x_r\rangle$ and $\langle y_r\rangle$

In the coordinate system for $\tilde{X}_r$, x_r is the distance between the ideal focal point given by Eq. 2. and the detector in the direction parallel to R. y_r is defined as being perpendicular to R and dependent on the divergence of the primary beam. An estimate of both these quantitites can be made following a method presented by H. Zantopulos and C. F. Jatczak[111] in which they compared the errors in parafocusing and stationary or non-focusing methods of residual stress analysis. Equations are derived for the path of the incident and diffracted beams. Defining the position of the PSD by an equation in the same coordinate system, the intersection of the diffracted beam and the PSD can be specified. The distance from the focus, point B in Fig. 1., to the intersection of the diffracted ray and the PSD can then be determined and x_r and y_r found.

---

*x_s is the displacement of the effective center of the diffracting volume from the center of the diffractometer.

The origin, 0, in Fig. 3. is the axis of rotation of the specimen and the cartesian coordinates ι, j define the equatorial plane. Assuming a flat sample, a primary beam divergence of 2α and 2φ as the observed Bragg angle, equations are derived for a divergent beam.

A. Equation for the incident beam.

In Fig. 3., the slope of the central incident beam is given by $-\cot\beta$, where $\beta=90-\varphi$. Using the law of sines in the triangle A0B to find the j axis intercept, the equations for the right and left incident beam are, respectively

$$j = -\cot(\beta-\alpha)\iota + R\sin\alpha/\sin(\beta-\alpha) \qquad 14.$$

$$j = -\cot(\beta+\alpha)\iota - R\sin\alpha/\sin(\beta+\alpha)$$

To generalize, let:

$\ell = 1$ for the right beam
$\ell = 0$ for the central beam
$\ell = -1$ for the left beam

Then the equation for the incident beam becomes

$$j = -\cot(\beta-\ell\alpha)\iota + \ell R\sin\alpha/\sin(\beta-\ell\alpha) \qquad 15.$$

B. Intersection of incident beam and specimen surface.

The specimen surface can be defined by:

$$j = \iota\tan\psi \qquad 16.$$

where ψ is defined in Fig. 1. Equating Eq. 15 and Eq. 16, the coordinates of the intersections are:

$$\iota_s = \frac{\ell R\sin\alpha/\sin(\beta-\ell\alpha)}{[\cot(\beta-\ell\alpha)+\tan\psi]} \qquad 17.$$

$$j_s = \iota_s\tan\psi \qquad 18.$$

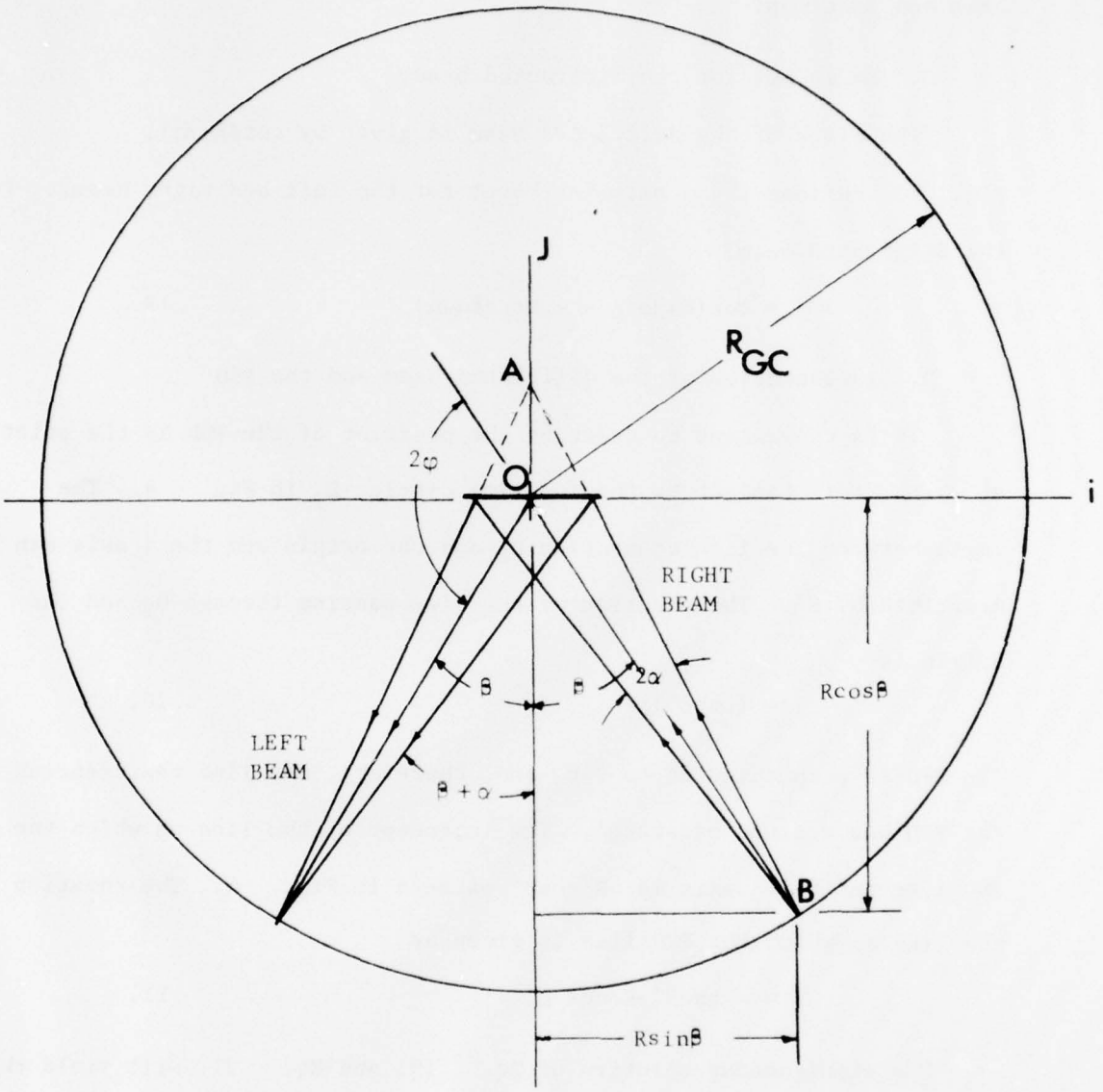

FIGURE 3 Geometry defining the angles of diffraction for the left and right divergent rays.

The subscript s in Eq. 18. refers to the intersection of the incident beam and specimen.

C. Equations for the diffracted beam.

The slope of the diffracted beam is given by $\cot(\beta+\ell\alpha)$. Fig. 3. defines the j axis intercept for the left and right beams. For the diffracted beam:

$$j = \cot(\beta+\ell\alpha)\iota - \iota_s\tan(\beta+\ell\alpha) \qquad 19.$$

D. Intersection of the diffracted beam and the PSD

It is convenient to describe the position of the PSD by the point at which it is tangent to the focusing circle, D_2 in Fig. 4. The angle between the line connecting D_2 and the origin and the j axis can be described by β'. The equation of the line passing through D_2 and the origin is

$$j = (\cot\beta')\iota \qquad 20.$$

The PSD is perpendicular to $0\text{-}D_2$ and, therefore, the line representing the PSD has a slope of $-\tan\beta'$. The intercept of the line on which the PSD lies and the j axis is $-R/\cos\beta'$ as seen in Fig. 4. The equation for the line on which the PSD lies is given by

$$j = -\iota\tan\beta' - R/\cos\beta' \qquad 21.$$

The simultaneous solution of Eq. 19. and Eq. 21. will yield the coordinates of Dl (the intersection of any diffracted beam and the PSD).

$$\iota_D = (\iota_s\tan(\beta+\ell\alpha) - R/\cos\beta')(1/(\cot(\beta+\ell\alpha)+\tan\beta')) \qquad 22.$$

$$j_D = -\iota\tan\beta' - R/\cos\beta'$$

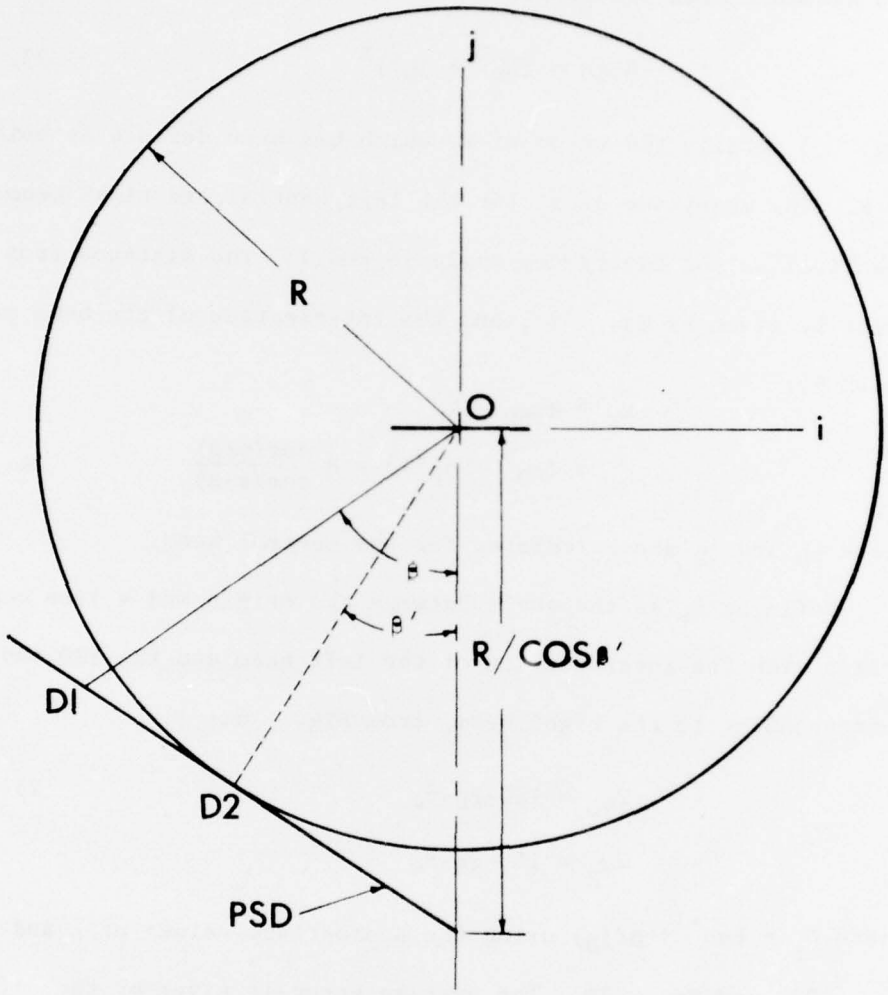

FIGURE 4 Geometry for the location of the position sensitive detector.

The distance from the sample to the detector is given by

$$R_{PSD} = (\iota_D^2 + j_D^2)^{\frac{1}{2}} \qquad 23.$$

Fig. 5 details the error of x_r which has been defined as being parallel to R. The magnitude of x_r for the left, central, and right beams are almost identical as the divergence angle is small. The distance from the focal point B, given by Eq. 2., and the intersection of the beam on the PSD is given by:

$$x_r \simeq R_{PSD} - R_P$$
$$= (\iota_D^2 + j_D^2)^{\frac{1}{2}} - R\,\frac{\cos(\psi+\beta)}{\cos(\psi-\beta)} \qquad 24.$$

where ι_D and j_D are calculated for the central beam.

Defining β_L as the angle between the origin and a line connecting the origin with the interesection of the left beam and the PSD and β_R similarly corresponding to the right beam, from Fig. 6.:

$$2\varphi_L = 180-\beta_L-\beta_c \qquad 25.$$

$$2\varphi_R = 180-\beta_R-\beta_c$$

where $\beta_\iota = \tan^{-1}(\iota_D/j_D)$ using the appropriate values of ι and j from Eq. 22. and Eq. 23. The average error is given by the difference between the angle of the central beam, $2\theta_c$, and the midpoint of the two extreme rays.

$$\Delta 2\varphi = 2\varphi_c - (2\varphi_c+2\varphi_R)/2 \qquad 26.$$

An average value of y_r is given by

$$\langle y_r \rangle = R_p \tan\Delta 2\varphi \qquad 27.$$

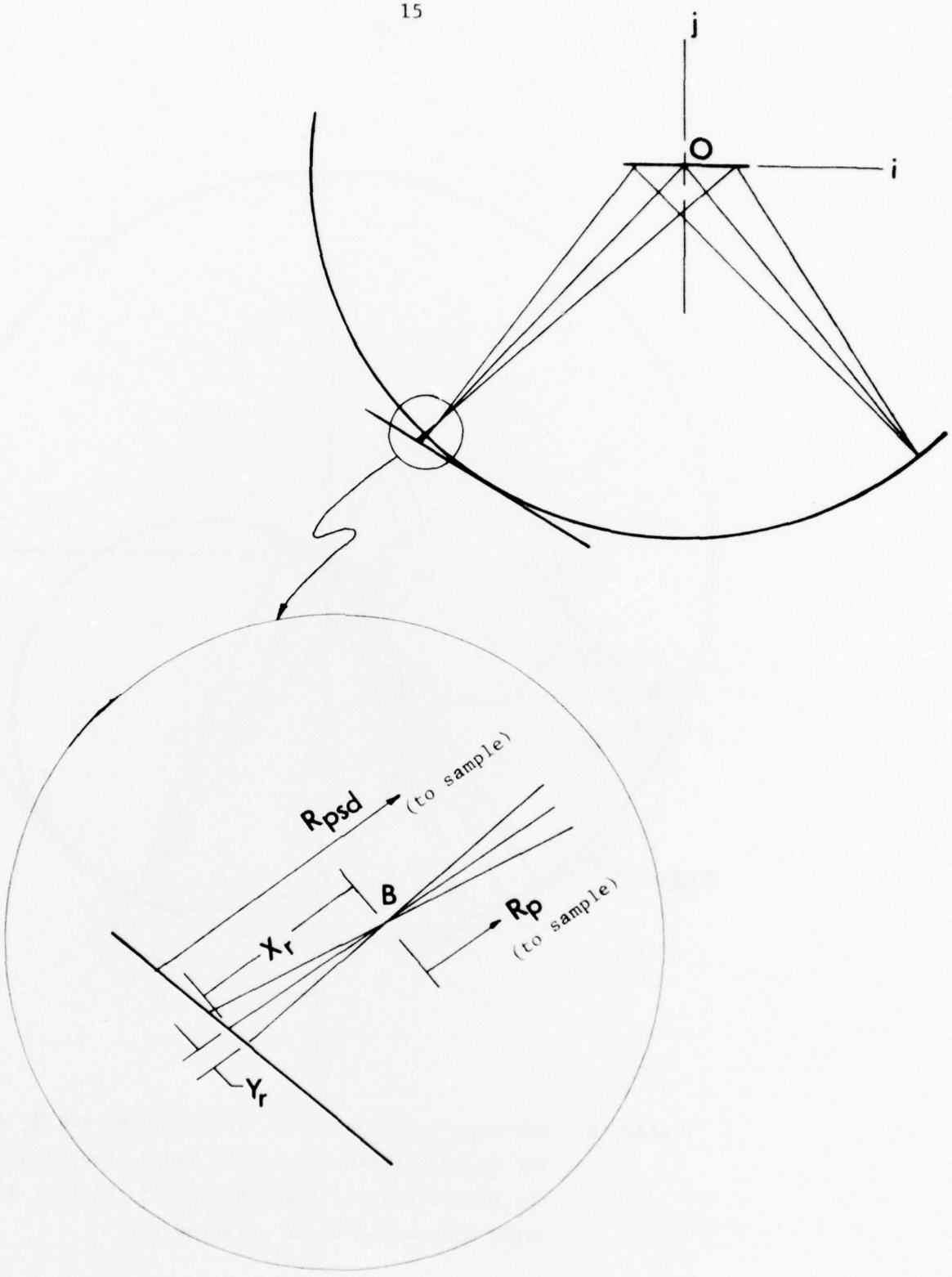

FIGURE 5 Geometry for x_r at $\psi=0^{\circ}$.

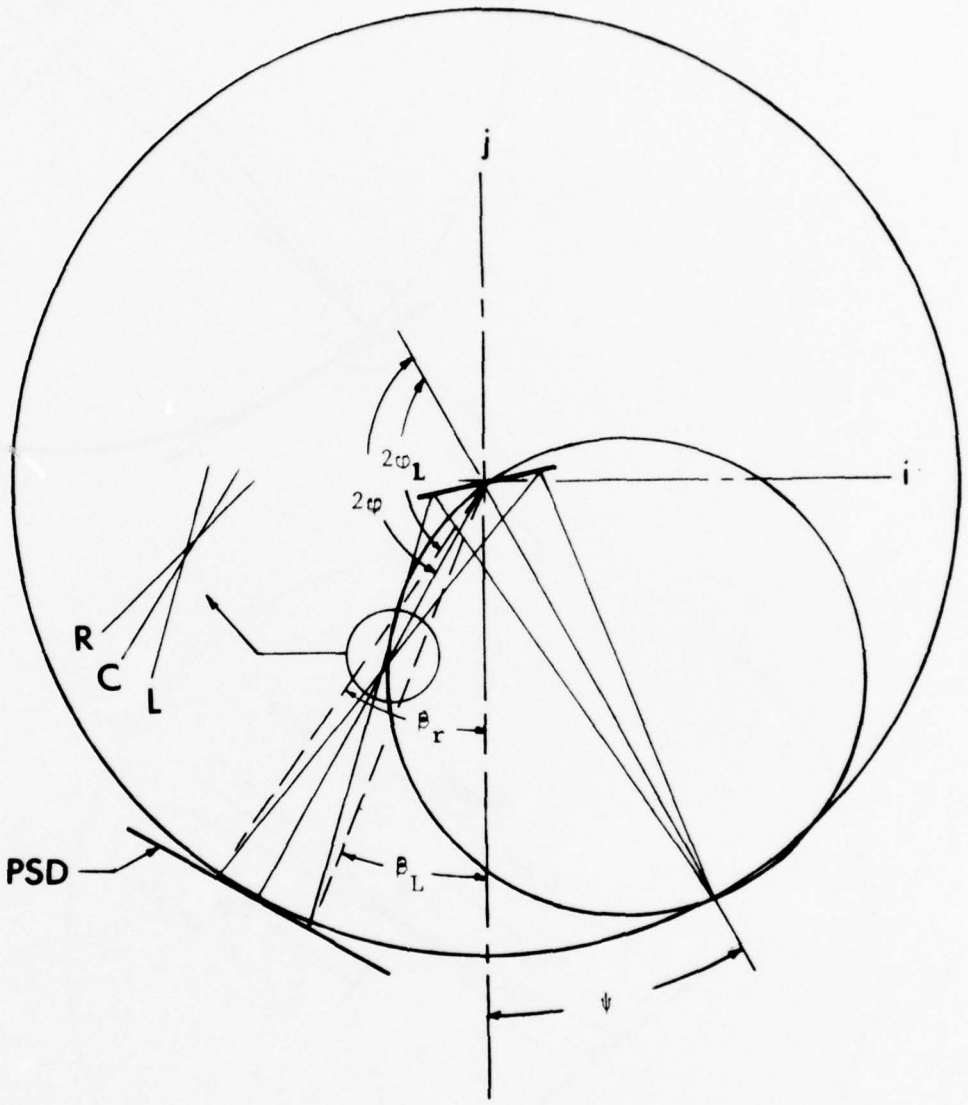

FIGURE 6 Geometry for y_r at $\psi=\psi^{\circ}$. The terms β_L and β_r describe the angle between the j axis and a line connecting the origin and the intersection of the left and right diffracted beams with the PSD.

It has been shown[111] the proper value is more like 1/3 of this average because the beam decreases in intensity rapidly on its edges. Eq. 27 is a very liberal estimate.

3 Results

The defocusing error is given by Eq. 13. The terms x_r and y_r pertaining to the distance of the PSD from the focusing circle are given by Eq. 24. and 27. respectively. The remaining terms $\langle x_s \rangle$ and $\langle y_s \rangle$ account for the interaction between the defocusing and sample position and a reasonable estimate of each must be used to determine the defocusing error.

An estimate of $\langle y_s \rangle$ is difficult as it depends on the alignment, however, Wilson[110] suggests a value of .25mm as the upper boundary. The term $\langle x_s \rangle$ represents the point of diffraction in the specimen. For CrK_α radiation this is less than .05mm in all cases.

The defocusing error was calculated assuming the center of the PSD is tangent to the $\psi=0^\circ$ focusing circle at $156^\circ 2\theta$. Table 1 tabulates the error assuming both $\langle x_s \rangle$ and $\langle y_s \rangle$ are zero for a radius of 14.55cm. The error, 2ε, in degrees is given for various values of the observed angle 2φ (column 1), ψ (column 2) and α (column 3). The error, 2ε, is given in column 4 and the true diffraction angle, 2θ, as given by Eq. 3. in column 5. The defocusing error is seen to be very small over the 10° range. In terms of stress for a peak shift from $154^\circ 2\theta$ at $\psi=0^\circ$ to $156^\circ 2\theta$ at $\psi=45^\circ$, representing a stress of opproximately 1200 MPa (174000 ksi), the error due to defocusing is only +2MPa(+290 psi) for a beam divergence (2α) of 2°. Table 2 tabulates the error for $\langle x_s \rangle$ = .05mm and $\langle y_s \rangle$ = .25mm. In this case the defocusing errors are larger, especially at $\psi=60^\circ$ because

TABLE 1

Defocusing Error for Position Sensitive Detector
PSD tangent to $\psi=0^\circ$ focusing circle at $156^\circ 2\theta$

($\langle x_s \rangle = 0$, $\langle y_s \rangle = 0$)

2θ (degrees)	ψ (degrees)	α (degrees)	2ε (degrees)	2θ (degrees)
150	0.0	0.5	0.0023	150.002
152	0.0	0.5	0.0022	152.002
154	0.0	0.5	0.0020	154.002
156	0.0	0.5	0.0019	156.002
158	0.0	0.5	0.0017	158.002
160	0.0	0.5	0.0015	160.002
150	0.0	1.0	0.0093	150.009
152	0.0	1.0	0.0087	152.009
154	0.0	1.0	0.0081	154.008
156	0.0	1.0	0.0074	156.008
158	0.0	1.0	0.0068	158.007
160	0.0	1.0	0.0062	160.006
150	45.0	0.5	0.0013	150.001
152	45.0	0.5	0.0013	152.001
154	45.0	0.5	0.0012	154.001
156	45.0	0.5	0.0012	156.001
158	45.0	0.5	0.0012	158.001
160	45.0	0.5	0.0011	160.001
150	45.0	1.0	0.0050	150.005
152	45.0	1.0	0.0050	152.005
154	45.0	1.0	0.0049	154.005
156	45.0	1.0	0.0048	156.005
158	45.0	1.0	0.0047	158.005
160	45.0	1.0	0.0045	160.005
150	60.0	0.5	0.0007	150.001
152	60.0	0.5	0.0008	152.001
154	60.0	0.5	0.0008	154.001
156	60.0	0.5	0.0009	156.001
158	60.0	0.5	0.0009	158.001
160	60.0	0.5	0.0009	160.001
150	60.0	1.0	0.0028	150.003
152	60.0	1.0	0.0031	152.003
154	60.0	1.0	0.0033	154.003
156	60.0	1.0	0.0034	156.004
158	60.0	1.0	0.0035	158.004
160	60.0	1.0	0.0036	160.004

TABLE 2

Defocusing Error for Position Sensitive Detector
PSD Tangent to ψ=0 focusing circle at 156°2θ

($\langle x_s \rangle$ = .05mm, $\langle y_s \rangle$ = .25mm)

φ (degrees)	ψ (degrees)	α (degrees)	2ε (degrees)	2θ (degrees)
150	0.0	0.5	0.0023	150.002
152	0.0	0.5	0.0022	152.002
154	0.0	0.5	0.0020	154.002
156	0.0	0.5	0.0019	156.002
158	0.0	0.5	0.0017	158.002
160	0.0	0.5	0.0015	160.002
150	0.0	1.0	0.0093	150.009
152	0.0	1.0	0.0087	152.009
154	0.0	1.0	0.0081	154.008
156	0.0	1.0	0.0074	156.008
158	0.0	1.0	0.0068	158.007
160	0.0	1.0	0.0062	160.006
150	45.0	0.5	- 0.0181	149.982
152	45.0	0.5	- 0.0167	151.983
154	45.0	0.5	- 0.0153	153.985
156	45.0	0.5	- 0.0139	155.986
158	45.0	0.5	- 0.0126	157.988
160	45.0	0.5	- 0.0122	159.989
150	45.0	1.0	- 0.0144	149.986
152	45.0	1.0	- 0.0130	151.987
154	45.0	1.0	- 0.0116	153.988
156	45.0	1.0	- 0.0103	155.990
158	45.0	1.0	- 0.0091	157.991
160	45.0	1.0	- 0.0079	159.992
150	60.0	0.5	- 0.0311	149.969
152	60.0	0.5	- 0.0292	151.971
154	60.0	0.5	- 0.0273	153.973
156	60.0	0.5	- 0.0254	155.975
158	60.0	0.5	- 0.0234	157.977
160	60.0	0.5	- 0.0214	159.979
150	60.0	1.0	- 0.0289	149.971
152	60.0	1.0	- 0.0269	151.973
154	60.0	1.0	- 0.0248	153.975
156	60.0	1.0	- 0.0228	155.977
158	60.0	1.0	- 0.0207	157.979
160	60.0	1.0	- 0.0187	159.981

of the correlation between the specimen and beam missettings with the receiving slit missetting. From Eq. 13. it can be seen that $\langle x_s \rangle$ is most important at $\psi=0$ where the cosine term is large and $\langle y_s \rangle$ is most important at $\psi=\psi^\circ$ where the sine term is large. Assuming the same 2° peak shift as before, the error in the peak shift between $\psi=0^\circ$ and $\psi=45^\circ$ is +4.2MPa (+600 psi), still a small error considering the large peak shift.

Table 3 tabulates the same quantities, $\langle x_s \rangle$ = .05mm and $\langle y_s \rangle$ = .25mm, for the PSD being tangent to the $\psi=0^\circ$ focusing circle at $139^\circ 2\theta$, a typical diffraction angle for the $Cr_{K\alpha}$ 311 diffraction plane in Al. The error is small for $\psi=0$ but is quite large at $\psi=45^\circ$ and $\psi=60^\circ$. This is because the sine term in Eq. 13. is large at this angle and the term $\langle y_s \rangle$ was .25mm. Assuming a peak shift from $139^\circ 2\theta$ to $141^\circ 2\theta$ using ψ tilts of 0° and 60° respectively, the error due to defocusing for Al, having a stress constant of 255 MPa/$^\circ 2\theta$ (37,000 psi/$^\circ 2\theta$) is -6.4 MPa (-920 psi). For $\langle y_s \rangle$ = 0, the defocusing error is less than .006$^\circ 2\theta$ at $\psi=45^\circ$. This effect is expected because at smaller 2θ, the effective sample positioning and beam alignment are more critical.

In summary, the defocusing error is small in the measurement of residual stress using the PSD and it is not necessary to apply mathematical corrections, especially if the X-ray tube is aligned properly so that the term $\langle y_s \rangle$ is small.

TABLE 3

Defocusing Error for Position Sensitive Detector
PSD tangent to $\psi=0^\circ$ focusing circle at $139^\circ 2\theta$

($\langle x_s \rangle$ = .05mm, $\langle y_s \rangle$ = .25mm)

2φ (degrees)	ψ (degrees)	α (degrees)	$2\epsilon_r$ (degrees)	2θ (degrees)
135	0.0	0.5	0.0036	135.004
137	0.0	0.5	0.0034	137.004
139	0.0	0.5	0.0033	139.003
141	0.0	0.5	0.0031	141.003
143	0.0	0.5	0.0029	143.003
145	0.0	0.5	0.0027	145.003
135	0.0	1.0	0.0144	135.015
137	0.0	1.0	0.0138	137.014
139	0.0	1.0	0.0131	139.013
141	0.0	1.0	0.0124	141.012
143	0.0	1.0	0.0117	143.012
145	0.0	1.0	0.0110	145.011
135	45.0	0.5	- 0.0279	134.972
137	45.0	0.5	- 0.0266	136.974
139	45.0	0.5	- 0.0253	138.975
141	45.0	0.5	- 0.0240	140.976
143	45.0	0.5	- 0.0226	142.977
145	45.0	0.5	- 0.0213	144.979
135	45.0	1.0	- 0.0237	134.976
137	45.0	1.0	- 0.0223	136.978
139	45.0	1.0	- 0.0208	138.979
141	45.0	1.0	- 0.0194	140.981
143	45.0	1.0	- 0.0181	142.982
145	45.0	1.0	- 0.0167	144.983
135	60.0	0.5	- 0.0421	134.958
137	60.0	0.5	- 0.0408	136.959
139	60.0	0.5	- 0.0394	138.961
141	60.0	0.5	- 0.0380	140.962
143	60.0	0.5	- 0.0365	142.964
145	60.0	0.5	- 0.0349	144.965
135	60.0	1.0	- 0.0407	134.959
137	60.0	1.0	- 0.0390	136.961
139	60.0	1.0	- 0.0373	138.963
141	60.0	1.0	- 0.0356	140.965
143	60.0	1.0	- 0.0338	142.966
145	60.0	1.0	- 0.0320	144.968

APPENDIX

Calibration Procedure

A position sensitive detector determines only the relative position of incomming photons in linear units along the detector. For X-ray diffraction studies, this relative position must be related to absolute units of the diffraction angle, 2θ. Three factors must be determined; 1) the absolute 2θ position of one point on the detector, 2) the relation between a fixed increment of distance along the detector to a 2θ increment, and 3) errors caused by the detector being flat rather than curved to the focusing circle of the diffractometer.

The third factor arises because in parafocusing geometry, the entire detector cannot be located at the true focal position. This produces a defocusing error in the determination of the real 2θ position. This problem is analyzed in depth in the main text and shown to be negligible, (an error of $.002^{\circ}$ was found when located 5° off the tangent to the focusing circle.)

The resolution between a fixed increment along the detector and the increment in degrees 2θ is not a constant quantity due to the curved focusing circle. Increments along the detector are measured in units of channels on the MCA from any reference position along the detector so that it is most convenient to calibrate the detector in terms of degrees 2θ per channel increment.

Referring to Fig. A.1 the angle 2φ is given by

$$2\varphi = \tan^{-1}\left(\frac{nz}{R}\right) \qquad (A.1)$$

where nz is the length along the PSD from the reference position, q, where q is taken as the point of tangency of the detector to the focusing

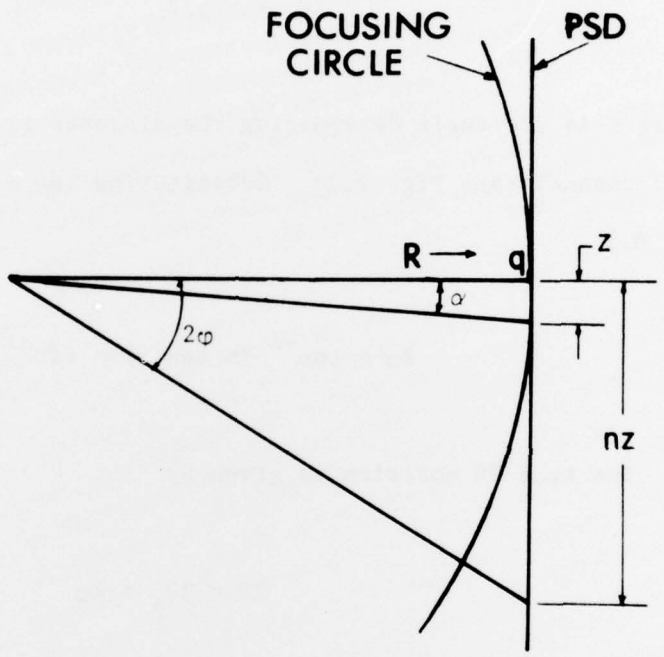

FIGURE A.1 Illustration of the terms used in the calibration of the PSD. The term 2φ represents the angular range covered by the detector, nz is the total number of channels and α is the angular increment for one channel, termed z, near the point of tangency of the PSD to the focusing circle.

circle. The distance from the center of the goniometer circle, R, is not known precisely because the position of the anode wire in the detector is difficult to determine. Also R and nz must be expressed in the same units (either channels or mm) which is inconvenient. It is practical in this case to eliminate R by defining a constant, k, such that

$$k = \alpha/z \tag{A.2}$$

where α is the angle determining the distance z, which can be made to be 1 channel (see Fig. A.1). Substituting $\tan \alpha = z/R$ and Eq. A.2 into Eq. A.1:

$$2\varphi = \tan^{-1} (n \tan \alpha) = \tan^{-1} (n \tan kz) \ . \tag{A.3}$$

The true 2θ position is given by

$$2\theta = 2\theta_o + 2\varphi \tag{A.4}$$

where $2\theta_o$ is the 2θ value for the point of tangency of the PSD to the goniometer circle.

By determining a calibration constant k in units of $^\circ 2\theta$/channel which is related to the conversion of distance (or channels) to angle near the point of tangency of the detector to the focusing circle, Eq. A.3 is subsequently used to calculate the angular position along the detector.

Calibration of the PSD requires two quantities, k and the position of q in terms of channel number. These were obtained in the following manner:

1) The 1090-1 sample exhibiting a sharp diffraction profile with excellent $K_{\alpha_1} - K_{\alpha_2}$ separation from the 211 planes was mounted

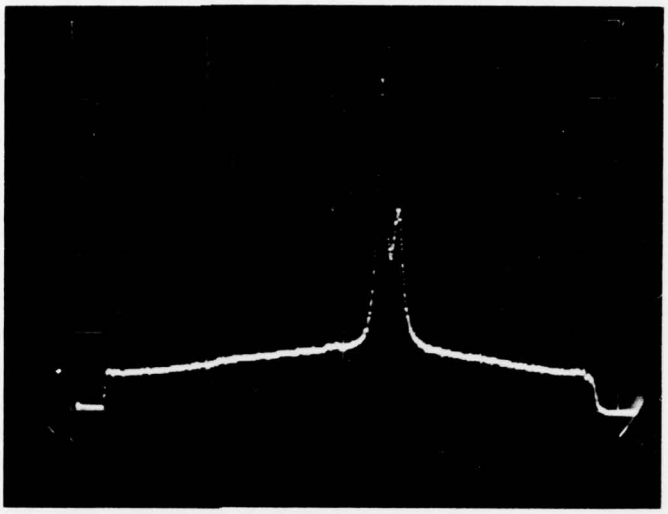

FIGURE A.2 Diffraction profile from 1090-1 sample.using the position sensitive detector. 211 peak, $\psi=0^{\circ}$, CrK_{α} radiation, 40KV-14mA, K_{β} filter, 1° divergent slit. The pattern was obtained in 100 seconds with the peak having 6107 counts.

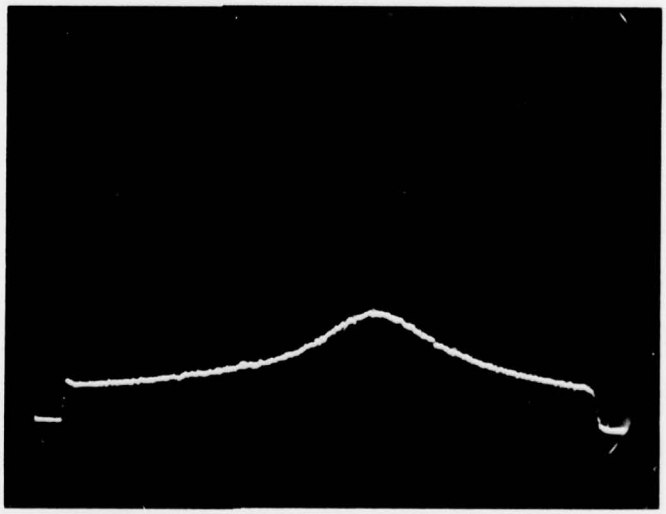

FIGURE A.3 Diffraction profile from the 1045-2 sample. Same parameters as in Fig. 2.10. The pattern was obtained in 100 seconds with the peak having 2155 counts.

and the 211 K_{α_1} and 211 K_{α_2} peak positions determined using the scintillation detector.

2) The 2θ arm was set to the 211 K_{α_1} 2θ peak position and the PSD was mounted. The position of the two 211 peaks were determined in terms of channel number. Figure A.2 shows the profile from this sample as obtained by the PSD.

The reference °2θ position, q, in terms of channel number is given by the K_{α_1} peak while the separation between the K_{α_1} - K_{α_2} peaks yield a value for k where z is taken as 1 channel. In this study k was usually .0202° 2θ/channel using 1024 channels for full storage of the PSD output in the MCA. Translating the detector perpendicular to the diffracted beam changes the absolute position, q, while moving the detector along the goniometer radius effects the calibration constant, k. Changes in the delay times (see Fig. A.4) on the crossover pickoffs will effect both k and q.

This calibration procedure is simpler than trying to apply Eq. A.1, because both the goniometer radius, R, and the conversion of channels into mm must be determined, neither of which is practical for rapid measurements.

To determine how serious is the non-linear relation between channels and °2θ, a comparison of the exact relation, Eq. A.3, to a constant calibration relation, $2\theta = 2\theta_o + k(nz)$ where k, n and z are as defined previously is given in Table A.1. For angles less than about 4° the approximation is accurate enough for peak determination. (The top 15% of a diffraction peak in the back reflection region is not usually greater than 6° wide or ± 3° from the tangency point.) Figure A.3 depicts the broad profile obtained from the 1045-2 sample. For other types of diffraction studies, notably small angle scattering, data may be

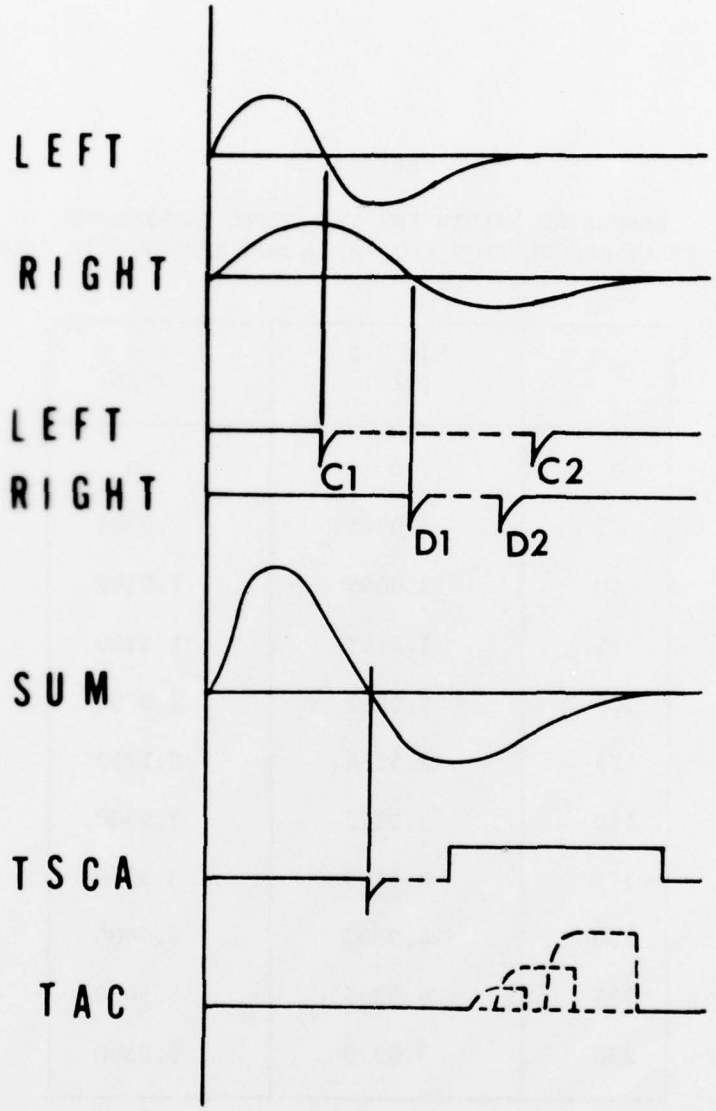

FIGURE A.4 Signal processing diagram depicting the timing sequence in determining the position of the incoming photon.

TABLE A.1

TABULATED VALUES FOR TWO THETA INCREMENTS
USING THE EXACT CALCULATION (EQ. A.3) AND APPROXIMATE CALCULATION*

N	Eq. 2.5 (°2θ)	K * N (°2θ)
0	0	0
25	.0505	.0505
50	1.0099	1.0100
75	1.5147	1.5150
100	2.0192	2.0200
125	2.5234	2.5250
150	3.0272	3.0300
175	3.5305	3.5350
200	4.0333	4.0400
225	4.5355	4.5450
250	5.0370	5.0500

*The calibration constant K was taken as .0202 °2θ/channel. N is the distance along the PSD (in terms of channels on the MCA) from the tangent point of the detector to the focusing circle (N=nz).

collected out to 7° or 8° 2θ from the point of tangency necessitating use of the exact formalization, unless R is made larger, say 1.5 times that for a standard diffractometer of radius 14.5 cm.

REFERENCES

108. Residual Stress Measurement by X-Ray Diffraction-SAE J 784a, 2nd Edition, Society of Automotive Engineers, Inc. (1971).

109. G. Kunze, A. Angew, Phys. 17, 412 (1964).

110. A. J. C. Wilson, Mathematical Theory of X-Ray Powder Diffractometry, Philips Technical Library (1963).

111. C. Jatczak and H. Zantopulos, Adv. in X-Ray Analysis, 14, 360 (1970).

Unclassified
Security Classification

DOCUMENT CONTROL DATA - R & D

(Security classification of title, body of abstract and indexing annotation must be entered when the overall report is classified)

1. ORIGINATING ACTIVITY (Corporate author)	2a. REPORT SECURITY CLASSIFICATION
J. B. Cohen, Northwestern University, Evanston, IL	Unclassified
	2b. GROUP

3. REPORT TITLE

(6) GEOMETRICAL PROBLEMS WITH A POSITION SENSITIVE DETECTOR EMPLOYED ON A DIFFRACTOMETER: ITS USE IN THE MEASUREMENT OF STRESS

4. DESCRIPTIVE NOTES (Type of report and inclusive dates)

(9) Technical Report No. 18

5. AUTHOR(S) (First name, middle initial, last name)

(10) M. R. James and J. B. Cohen

(11) 15 Jun 77

6. REPORT DATE	7a. TOTAL NO. OF PAGES	7b. NO. OF REFS
(15) N00014-75-C-0580	~~30~~ (12) 37	4

8a. CONTRACT OR GRANT NO	9a. ORIGINATOR'S REPORT NUMBER(S)
5345-455	Technical Report No. 18 (14) TR-18
b. PROJECT NO.	
c.	9b. OTHER REPORT NO(S) (Any other numbers that may be assigned this report)
d.	None

10. DISTRIBUTION STATEMENT

Distribution of this document is unlimited.

11. SUPPLEMENTARY NOTES	12. SPONSORING MILITARY ACTIVITY
	Office of Naval Research Metallurgy Branch

13. ABSTRACT

Defocussing errors associated with the use of a straight one dimensional position sensitive detector on a diffractometer are examined. Over a $10^{\circ}2\theta$ range the error is $0.02^{\circ}2\theta$ at worst.

260810

DD FORM 1 NOV 65 1473 (PAGE 1)

S/N 0101-807-6801

Unclassified
Security Classification

14 KEY WORDS	LINK A		LINK B		LINK C	
	ROLE	WT	ROLE	WT	ROLE	WT
X-Ray Stress Measurement						
Position Sensitive Detector						
PSD						